SLAC-PUB-500
September 1968
(ACC)

USE OF THERMOLUMINESCENT DOSIMETERS IN HIGH ENERGY HEALTH PHYSICS*

G. K. Svensson, R. C. McCall, T. M. Jenkins, and W. R. Nelson
Stanford Linear Accelerator Center
Stanford University, Stanford, California

ABSTRACT

The use of thermoluminescent dosimeters around a 20-GeV electron accelerator is discussed. Advantages over other types of dosimeters, problems of calibration and interpretation of results, and fabrication techniques are described. Application to the measurement of electromagnetic showers, electron and muon scattering, bremsstrahlung distributions, beam profiles, etc. are presented.

(Presented at the 2nd International Conference on Luminescence Dosimetry, September 23-26, 1968, Gatlinburg, Tennessee.)

*Work supported by the U.S. Atomic Energy Commission.

INTRODUCTION

The usual advantages of thermoluminescent dosimeters — small size, low cost per dosimeter, wide dynamic range, etc. — are of even more value around high energy electron accelerators. Areas to be covered in a series of measurements are very large — the research yard at SLAC, for example, is over a half million square feet. Dose distributions are apt to show very strong angular dependences. For example, a 1-GeV electron beam striking a thin target will produce a bremsstrahlung beam whose intensity will drop to one half at about one tenth of a degree. Measurements of photon dose rates around a thick (e.g., 9 inches copper — 15.6 radiation lengths) target struck by an electron beam in the GeV range vary by an order of magnitude from 15^{o} to 180^{o}. At smaller angles, the variation is much faster with angle, dropping an order of magnitude in about 5^{o}. In addition the relative independence of environmental conditions is of great value. Many of our measurements are made outdoors in conditions ranging from 30^{o} F to 100^{o} F and from extreme dryness to torrential rains. Indoor measurements are often made in high rf and magnetic fields and conditions requiring 1-2 weeks delay before the dosimeters are recovered. Measured doses range from 10^{5} rad to a few mrads. Thermoluminescent dosimeters have performed well under all of these conditions.

For all of our measurements we have used lithium fluoride although we have available some CaF_2:Mn dosimeters. Because of our wide range of applications we have used most forms of lithium fluoride. Loose powder has been used most because of its versatility, low cost, and good reproducibility. We also use LiF in the form of teflon discs,* teflon rods,* extruded rods,** and extruded ribbons**.

---

* Isotopes, Inc. (ConRad), Westwood, New Jersey.

** Harshaw Chemical Company, Cleveland, Ohio.

For different applications, each of these dosimeter forms have certain advantages. We will describe some of the applications in the following paragraphs.

CALIBRATION PROCEDURE

The energy distribution of the radiation field as well as particle-type distribution varies strongly around the accelerator. The properties of LiF regarding photon energy dependence over a wide energy range and relative mass stopping power variation will be shown in two experiments — the muon experiment and the water shower experiment. They will be shown to meet the requirements for evaluating absorbed dose in low-Z materials (water, plastics and tissue-equivalent materials).

Calibration of the TLD is being done on a ^{60}Co source installed in a concrete well. The source is often collimated to reduce the scattered contribution from the concrete walls. From measurements of exposure (Victoreen condenser ion chambers) the absorbed dose in the medium in which the TLD is inserted can be calculated. In general, dosimeters of the size we use, usually ranging from 0.4 mm-1 mm, will perturb the flux of secondary particles in this medium whether it be an experimental medium or a calibration medium. For example, 1.25 MeV photons will give rise to a mean initial Compton electron energy of 0.65 MeV. These have ranges of the order of 1 mm in pure LiF. The consequence is that the dosimeter response is the combined effect of the absorbed dose in the medium and in the dosimeter itself.

Burlin[1] has developed a modified cavity chamber theory to correct for this which applies to the described situation. He shows, however, that the difference in response between a small cavity and a cavity with linear dimensions equal to the range of the directly ionizing particles is small when the atomic numbers of cavity and wall do not differ appreciably. Since the dosimeters we use have

approximately the same atomic number and hence the same mass absorption coefficient and the same electron density ($\sim 2.8 \times 10^{23}$ electrons/g) and therefore the same mass stopping power as the medium in which they most often are used, we have not applied any corrections for this effect.

In the shower experiment described below the dosimeters were placed in lead and copper and the discussion above does not apply with this large difference in atomic number. The thickness of our dosimeters was about equal to the range of a 0.5 MeV electron. It is difficult to estimate how large an error this produces. Monte Carlo calculations give some insight into the matter. For a 1-GeV electron in lead, $\sim$ 30% of the energy is deposited by electrons and photons initially having energies less than 1 MeV. A very rough estimate indicates that $\sim$ 15% of the energy would be deposited by electrons and photons initially below 0.5 MeV and Burlin indicates we might measure this portion $\sim$ 50% too low. Then our results would be something like 8% too low overall. This analysis is inadequate but is the best we are able to do until further experiments or Monte Carlo studies are available.

APPLICATIONS

Shower Experiments

There had been many calculations of the electromagnetic shower development but no experimental measurements at the energies of interest when our accelerator was being built. It was decided to perform such an experiment using thermoluminescent dosimeters. These measurements, which have been previously reported[2,3], were done in the geometry shown in Fig. 1. The detectors are LiF packed in teflon tubing with an inner diameter of 0.023 inches. LiF will flow into such tubing easily if vibrated with something such as an engraving tool. During readout, small sections were cut off and the LiF vibrated out and weighed.

It was possible to handle sections as small as 1.85 mm containing 0.9 mg of phosphor. Typical results are shown in Figs. 2 and 3 for longitudinal and radial shower distributions, respectively. For the longitudinal case where the variation was rather slow with depth our geometric resolution was excellent. For the radial distribution, however, we were limited by the size of our detectors. The exposure was made with two pulses from the Stanford Mark III accelerator. Approximately 4000 points were measured.

Electron Scattering Experiment

Early in the operation of the two-mile accelerator, it was found necessary to limit the beam current in certain experiments because of resulting radiation levels. These were found to be caused by scattered electrons striking the beam transport pipe. High energy scattering had been theoretically described by Molière[4] and Nigam et al.[5] and Marion and Zimmerman[6] but experimental confirmation was lacking except at very small angles. An experiment was performed to measure the distribution. The detector arrays used are shown in Fig. 4. These are lucite plates with grooves and holes machined to hold LiF detectors. The inner square array holds 1 mm diameter extruded rods and the circles hold lengths of tubing similar to those described above. The extruded rods were chosen over teflon rods because of slightly better reproducibility — one standard deviation = ± 2% as compared with ± 3%. Several of these arrays were exposed sequentially at a fixed distance from different thicknesses of scattering targets. The result is shown in Fig. 5.[7] The abscissa is in units proportional to the scattering angle where X = 10 corresponds to an angle of about 5.5 milliradians. The divergence of our measured points from theory does not conclusively show that the theory is inadequate at large angles since it is possible that the electron beam contained scattered components before

striking the target. It does indicate, however, how calculations of electron scattering can underestimate the resulting radiation fields and the amount of shielding necessary.

Muon Experiment

In many applications at SLAC the limitations on forward shielding are set by the muon dose rate. For example, a 20 GeV electron beam of 200 kW stopped in a target gives a dose rate of 2 rem/hour at 100 meters in the zero degree direction. To decrease this by a factor of 10 requires over 150 feet of earth shielding. The angular distribution of the muon dose rate after a thick shield is influenced by multiple scattering. Again, no experimental verification of theory was available at the energies we were interested in. An experiment was performed using detector arrays identical to those in Fig. 4.[8] The muon dose distribution from an 18-GeV electron beam striking a copper dump was measured after penetrating 14 feet of iron. The results are shown in Fig. 6. The difference in shape between the experimental and theoretical curves is believed due to neglect in the theory of nuclear form factors and the fact that the photons producing the muons have an angular distribution. However, the total energy deposited from the muon beam should be the same in the theoretical and experimental case, if the TLD correctly read absorbed dose, that is, if our calibration procedure is satisfactory. An integration over the two curves ($2\pi \int_0^\infty r\, D(r)\, dr$, where D(r) is calculated or measured absorbed dose at radius r from beam center) gives a difference that is within the estimated error limits. Measured points and the calculated curve have the same maximum error of ± 10%.

Water Shower Experiment

An accelerator health physicist is faced with the possibility of trying to assess the dose of a person struck by the beam. One necessary piece of data

is the resulting dose distribution in the body. To measure this distribution, an experiment was performed with the geometry shown in Fig. 7.

A lucite tank 2' × 2' and 1' thick was filled with water. Six detector arrays such as those used for the described electron scattering experiment were inserted at different depths. The large amount of dosimetric data is still being evaluated but some interesting results have appeared from the front plate. This plate is attached next to the inside wall of the tank, which has a wall thickness of 1/2 inch. The dose in the center of this plate is mainly due to the primary electron beam (10 GeV) since we can assume there is no significant dose build-up due to electromagnetic shower development at that depth (1/2-inch lucite $\simeq 0.05$ radiation lengths). Accordingly we can let the radial dose distribution illustrate the beam profile. Figure 8 shows the beam profile in two dimensions. The dose in the outer rods is probably due to secondary effects, e.g., backscattering, penumbra, etc. The beam profile was also measured with glass slides and these data have been normalized to the histogram. The thermoluminescent dosimeters allow measurement over a greater range (4-5 decades compared with 1-2 decades) than the commonly used glass slides, as well as capability of measuring beam profiles for much lower beam intensities.

The elliptical beam spot is typical at the place the experiment was performed. During this experiment the electron beam was monitored very accurately and we know that the total number of electrons was $6.15 \times 10^9 \pm 1\%$ (S.D.). Looking only at the center rod we can calculate the number of electrons entering that rod.

By making the reasonable assumption that the elliptical beam has a profile of Gaussian shape along either semi-axis, we can derive an expression for the fraction F of the electrons entering the center rod (0.5 mm radius).

$$F = \frac{\int_0^R \int_0^{\pi/2} r\, e^{-t(r,\theta)}\, dr\, d\theta}{\int_0^\infty \int_0^{\pi/2} r\, e^{-t(r,\theta)}\, dr\, d\theta}$$

where $t(r, \theta)$ involves the elliptic equation in polar coordinates and is given by

$$t(r, \theta) = \frac{r^2}{a^2 b^2} (b^2 \sin^2 \theta + a^2 \cos^2 \theta)$$

$$= \frac{r^2}{a^2 b^2} \left[(b^2 - a^2) (1 - \cos 2\theta)/2 + a^2 \right]$$

where b = semi-major axis, a = semi-minor axis. The integration over the angle θ yields the final expression

$$F = \frac{\int_0^R r\, e^{-(a^2 + b^2)P} I_0(P)\, dr}{\int_0^\infty r\, e^{-(a^2 + b^2)P} I_0(P)\, dr}$$

where $I_0(P)$ is the Bessel function of degree n = 0 and with argument $P = \frac{r^2}{a^2 b^2}$. For R = 0.5 mm, a = 0.48 mm and b = 1.33 mm, the solution is F = 0.40. The particle fluence ϕ in the center rod is

$$\phi = \frac{0.40 \times 6.15 \times 10^9}{\pi (5 \times 10^{-2})^2} \quad \frac{\text{electron}}{\text{cm}^2}$$

The choice of collision mass stopping power was made by using data from Berger-Seltzer[9] which are given up to a maximum energy of 1 GeV. An extrapolation from 1 GeV to 10 GeV yields

$$\left(\frac{1}{\rho} \frac{dT}{dX} \right)_{\text{LiF}}^{10\ \text{GeV}} = 2.14 \quad \frac{\text{MeV - cm}^2}{\text{gm}} .$$

The absorbed dose in the center rod is

$$D = \frac{0.40 \times 6.15 \times 10^9}{\pi (5 \times 10^{-2})^2} \quad \frac{\text{electrons}}{\text{cm}^2} \times 2.14 \times 1.6 \times 10^{-6} \quad \frac{\text{erg - cm}^2}{\text{g}} \times \frac{10^{-2}\ \text{rad g}}{\text{erg}}$$

$$= 1.07 \times 10^4 \text{ rads.}$$

The measured value in the center rod is

$$1.08 \times 10^4 \text{ rad} \pm 5\% \text{ S.D.}$$

The collision mass stopping power includes the energy transfer which creates high energy δ rays, especially in the case of electron-electron interaction. Since these δ rays might transport part of the transferred energy out of the detector volume, the calculated dose ought to be an over-estimation. Using a restricted LET would have been the correct way of calculating the dose, but we have not yet evaluated the importance of that concept.

For a similar purpose, we have attempted to develop a method of determining the dose to a person standing near a spot where there is a beam loss, e.g., a slit or collimator or a target.[10] The method chosen was to irradiate an Alderson phantom* under such conditions and measure the induced activity resulting. This method had been used by others[11, 12, 13] previously for heavy particle accelerators. For an electron accelerator, the major induced activities are ^{11}C and ^{15}O. Of these two isotopes, only the ^{11}C is long-lived enough for useful measurement. At longer times after exposure, ^{24}Na and ^{7}Be are measurable. The bremsstrahlung is the dominant radiation component for both dose and activation and was measured primarily by thermoluminescent dosimeters placed within the phantom.

Effective Energy Measurements

Sometimes we encounter relatively intense photon beams in checking out new beam transport arrangements. It is of interest to both Health Physics and the experimenter to know the origin of these photons which could, for example, be high energy bremsstrahlung, medium energy scattered bremsstrahlung, or low energy (< 1.0 MeV) synchrotron radiation. An exposure of several thermoluminescent dosimeters between a series of lead absorbers gives a reasonably good, quick answer. Other detectors could, of course, be used for this purpose.

*Alderson Research Labs., Long Island City, New York.

The advantage here is economy of beam time and ease of making an exposure that falls within the dynamic range of the dosimeter.

Personnel Dosimetry

SLAC is also using thermoluminescent dosimeters for visitors' personnel dosimeters. A simple badge* holding a ^{7}LiF and ^{6}LiF teflon disc is used. Since the number of badged visitors ranges from 1000-1500/month, there is a saving of about $1000/month available. Eventually we expect to replace film badges with thermoluminescent dosimeters for employees also. Employees presently carry a wallet card containing a ^{7}LiF teflon disc as an emergency and supplementary dosimeter.

*Radiation Detection Company, Mountain View, California.

REFERENCES

1. T. E. Burlin, "Cavity Chamber Theory" in Radiation Dosimetry Vol. 1, Frank H. Attix and William C. Roesch editors (Academic Press, 1968).
2. T. M. Jenkins, J. K. Cobb, W. R. Nelson and R. C. McCall, "Measurement of Electron-Induced Showers with Thermoluminescent Dosimeters," Nucl. Instr. and Methods 37, 174-175 (1965).
3. W. R. Nelson, T. M. Jenkins, R. C. McCall and J. K. Cobb, "Electron-Induced Cascade Showers in Copper and Lead at 1 GeV," Phys. Rev. 149, 201-208 (1966).
4. G. Molière, Z. Naturf 2a, 133 (1947); Z. Naturf 3a, 78 (1948).
5. B. P. Nigam, M. K. Sundaresan, and T. Y. Wu, "Theory of Multiple Scattering: Second Born Approximation and Corrections to Molière's Work," Phys. Rev. 115, 491 (1959).
6. J. B. Marion and B. A. Zimmerman, "Multiple Scattering of Charged Particles," Nucl. Instr. and Methods 51, 93 (1967).
7. T. M. Jenkins and W. R. Nelson, "The Effect of Target Scattering on the Shielding of High Energy Electron Beams," Report No. SLAC-PUB-432, Stanford Linear Accelerator Center, Stanford University, Stanford, California, (1968); to be submitted to Health Physics.
8. W. R. Nelson, "The Shielding of Muons Around High Energy Electron Accelerators: Theory and Measurement," Report No. SLAC-PUB-481, Stanford Linear Accelerator Center, Stanford University, Stanford, California, (1968); to be submitted to Nucl. Instr. and Methods.
9. M. J. Berger and S. M. Seltzer, "Additional Stopping Power and Range Tables for Protons, Mesons, and Electrons," NASA SP 3036 (1966).

10. T. M. Jenkins and R. C. McCall, "Emergency Determination of Dose Equivalent in High Energy Accelerator Accidents," Report No. SLAC-PUB-447, Stanford Linear Accelerator Center, Stanford University, Stanford, California, (1968).

11. G. Legeay, L. Court, L. Prat, L. Jeanmaire, J. L. Daburon, H. DeKerviler, and P. Tardy-Joubert, "Dosimetrie des Protons de Haut Energie par Mesure de Beryllium-7 Forme dans les Tissus," in Personnel Dosimetry for Radiation Accidents, International Atomic Energy Agency, Vienna (1965); p. 507.

12. M. M. Kamochkov, "Estimation of the Dose From Accidental Irradiation by a Large Amount of High Energy Particles," CERN TRANS-66-5, Original JINR Report P-2008 (1965).

13. M. Barbier, A. Hutton and A. Pasinetti, "Radioactivity Induced in Tissue by 600 MeV Protons," CERN 66-34 (1966).

FIGURE CAPTIONS

1. Copper absorber used in electromagnetic shower experiment showing the relative positions of LiF detector strings.
   (a) Exploded view; (b) assembled view.
2. Longitudinal energy deposition in lead. A comparison of this experiment with a Monte Carlo calculation.
3. Energy deposition profile curves for 1 GeV electrons incident upon copper. Measured points are shown for a representative depth. Errors are slightly larger than shown by data circles.
4. Lucite plates used as a detector holder for TLD rods (small holes) and TLD strings (rings). Array in center holds 81 TLD rods.
5. Comparison of the measured and theoretical distribution function, F(X), for a 10 GeV positron beam incident upon a 0.1 radiation length copper target. The solid line is the theoretical calculation of Marion and Zimmerman;[6] the dashed line was drawn through the data by eye.
6. Comparison of measured and theoretical muon dose distributions (with and without multiple scattering) for an 18.0 GeV electron beam separated from a detector by 14.0 feet of iron.
7. Lucite tank with six detector plates used for measurement of longitudinal and radial dose in water.
8. Electron beam profile during water shower experiment measured by TLD extruded rods (histogram), and by glass slide exposure (solid line) normalized to TLD data. One standard deviation for TLD data is $< 5\%$ for all points.
   (a) Horizontal profile; (b) vertical profile.

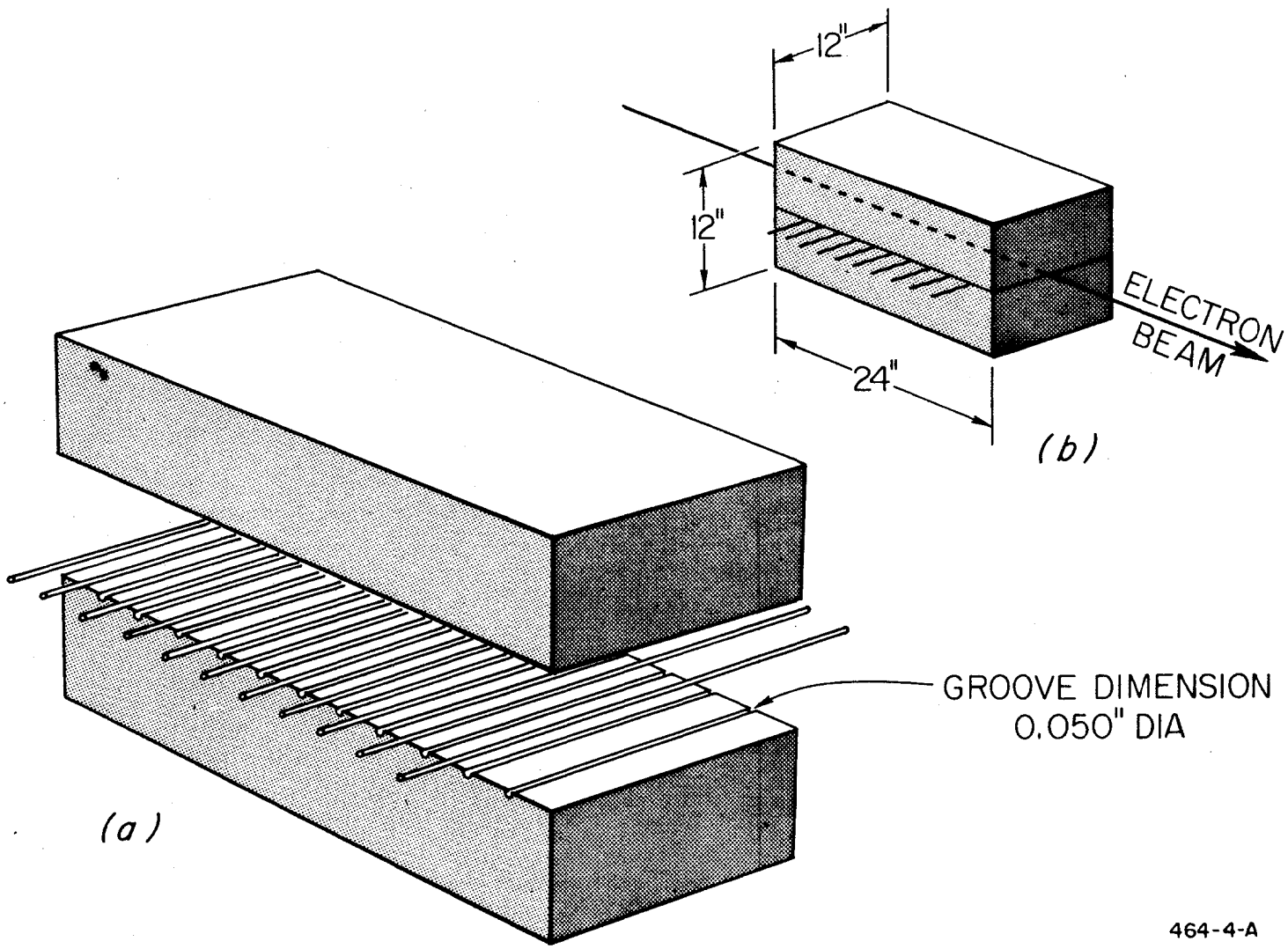

Fig. 1

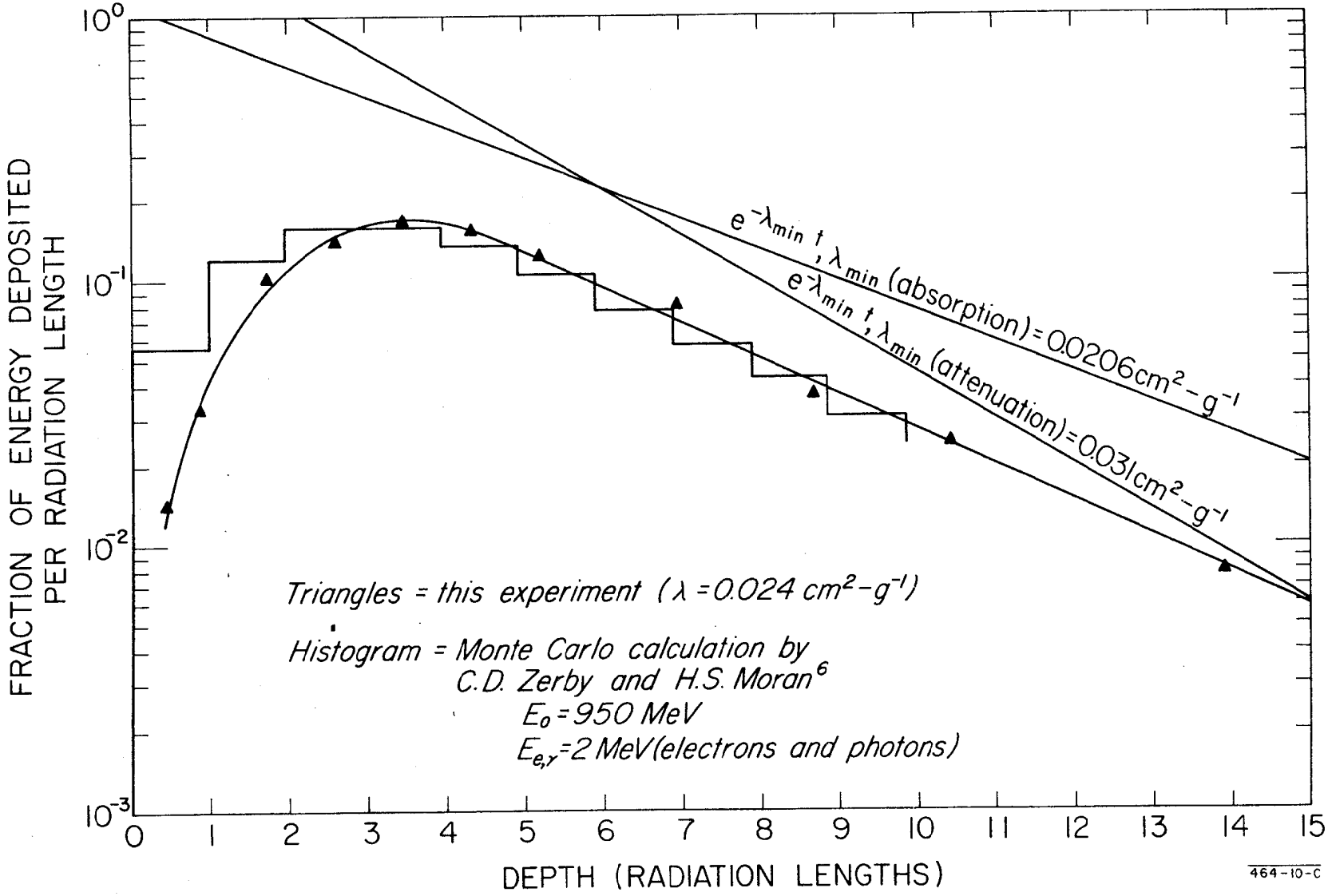
FRACTION OF ENERGY DEPOSITED PER RADIATION LENGTH
10^0
10^{-1}
10^{-2}
10^{-3}
0 1 2 3 4 5 6 7 8 9 10 11 12 13 14 15
DEPTH (RADIATION LENGTHS)
$e^{-\lambda_{min} t}, \lambda_{min}$ (absorption) = 0.0206 cm^2-g^{-1}
$e^{-\lambda_{min} t}, \lambda_{min}$ (attenuation) = 0.031 cm^2-g^{-1}
Triangles = this experiment (λ = 0.024 cm^2-g^{-1})
Histogram = Monte Carlo calculation by
C.D. Zerby and H.S. Moran[6]
E_o = 950 MeV
$E_{e,\gamma}$ = 2 MeV (electrons and photons)
464-10-C

Fig. 2

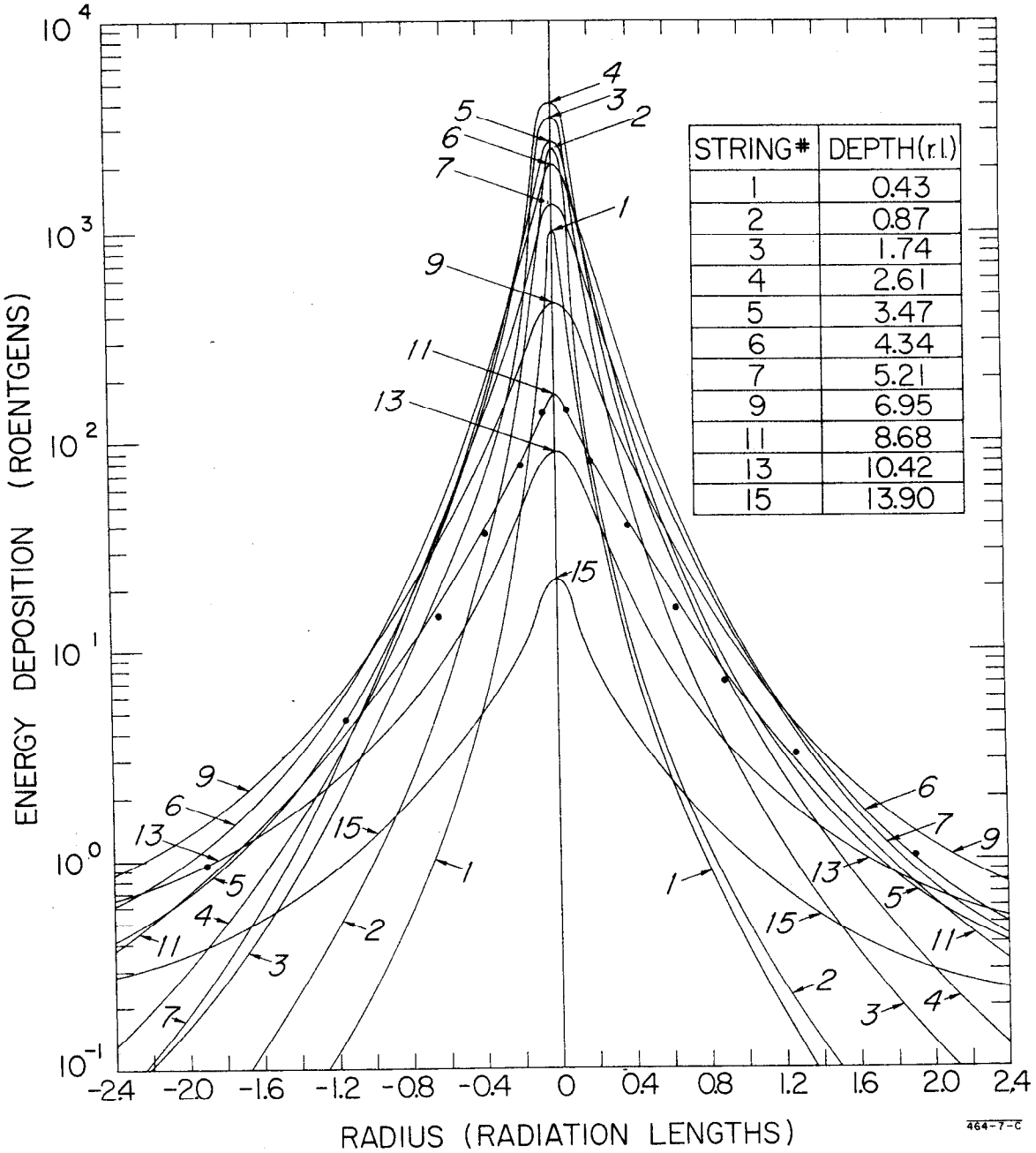
ENERGY DEPOSITION (ROENTGENS)
RADIUS (RADIATION LENGTHS)
STRING# | DEPTH(r.l.)
1 | 0.43
2 | 0.87
3 | 1.74
4 | 2.61
5 | 3.47
6 | 4.34
7 | 5.21
9 | 6.95
11 | 8.68
13 | 10.42
15 | 13.90
464-7-C

Fig. 3

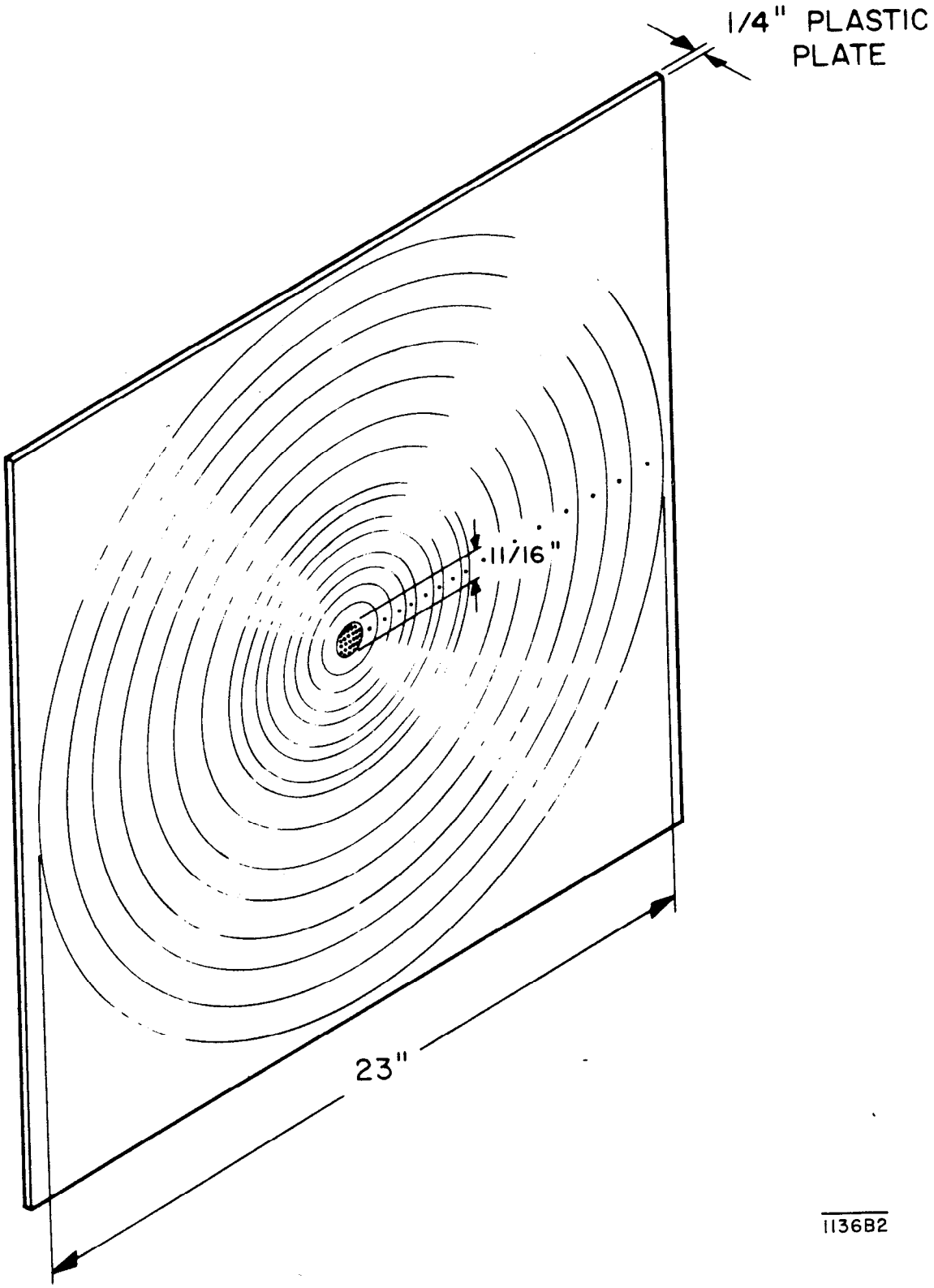

Fig. 4

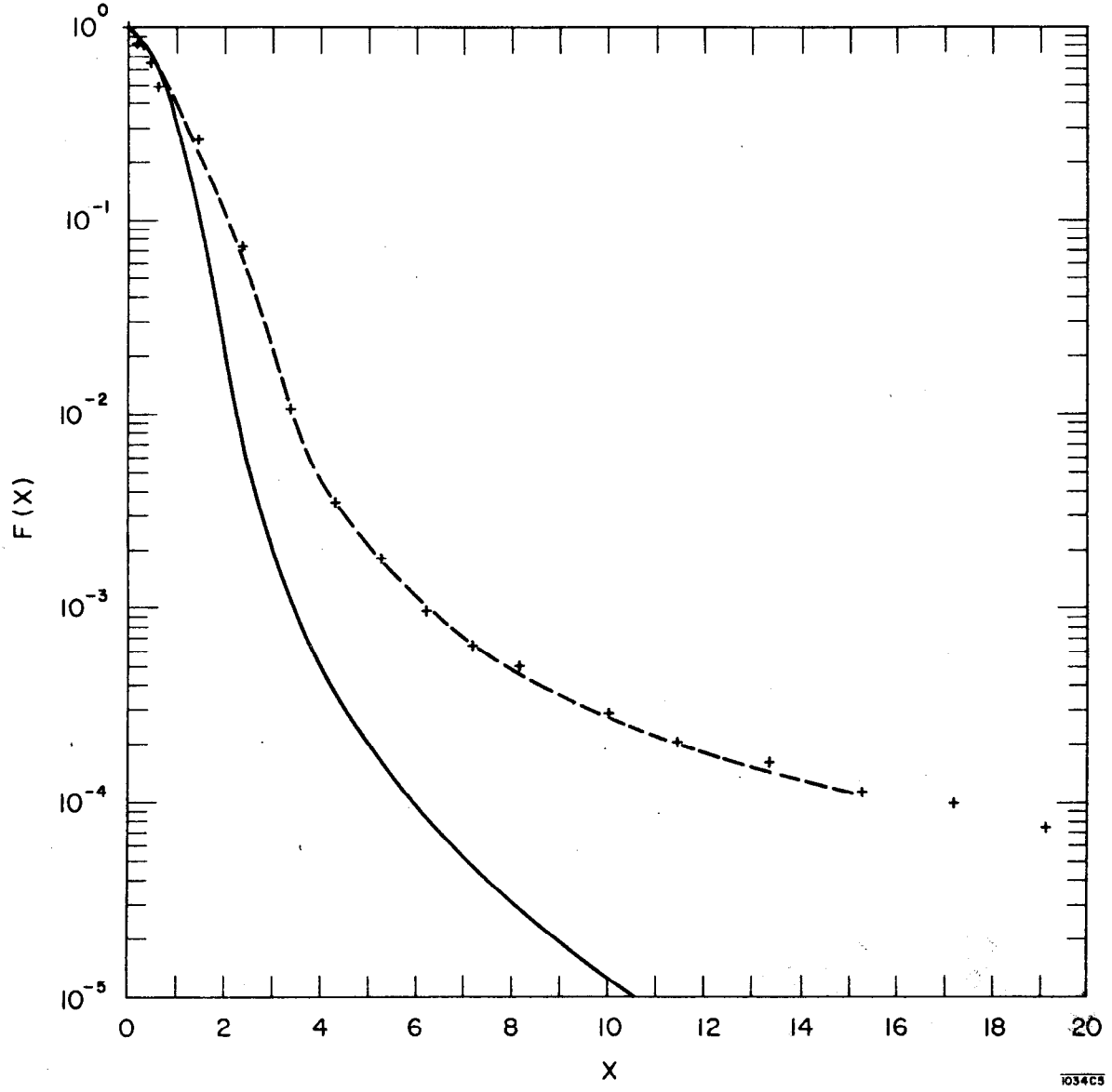

Fig. 5

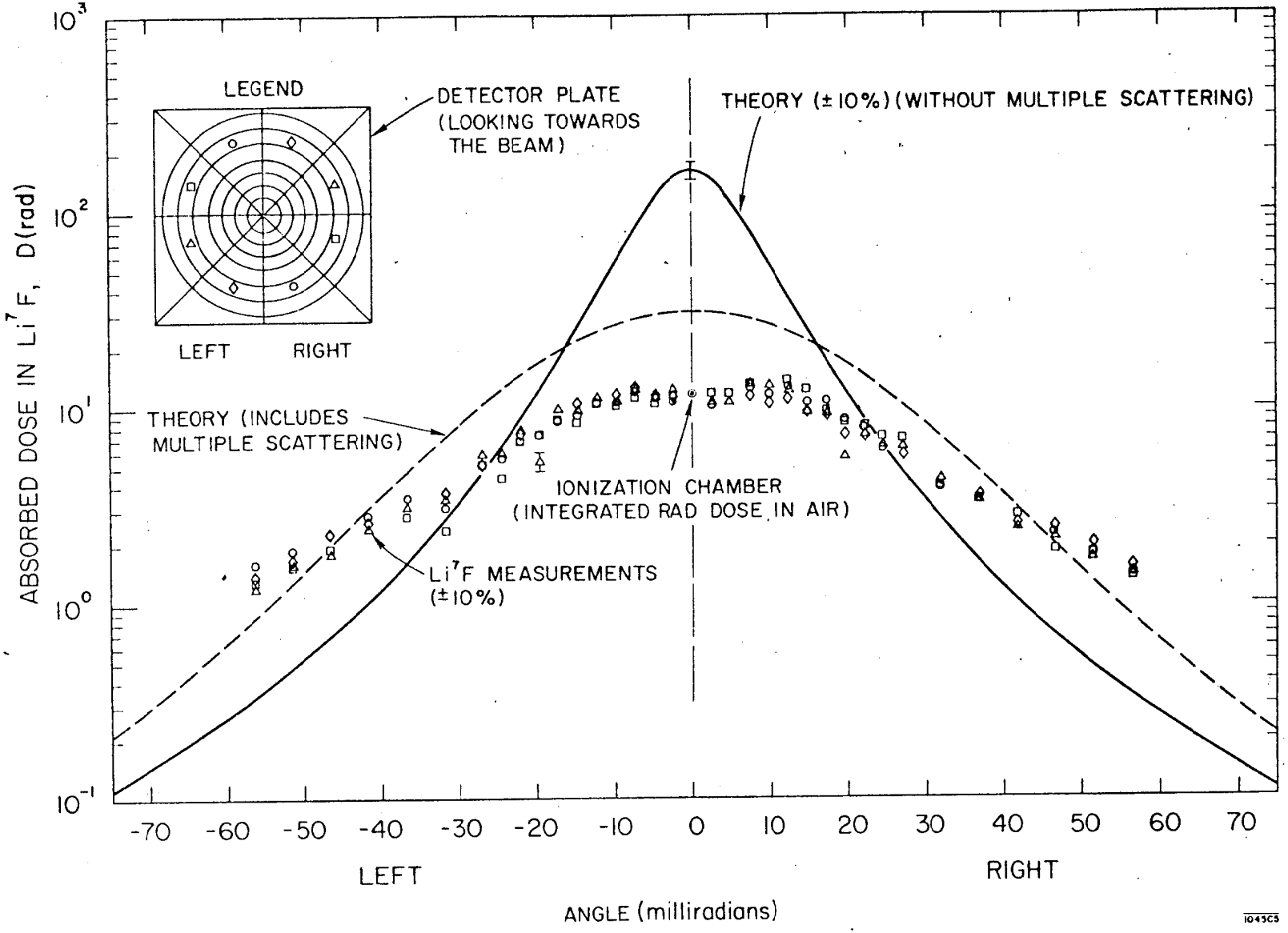
LEGEND
DETECTOR PLATE (LOOKING TOWARDS THE BEAM)
LEFT
RIGHT
THEORY (±10%) (WITHOUT MULTIPLE SCATTERING)
THEORY (INCLUDES MULTIPLE SCATTERING)
IONIZATION CHAMBER (INTEGRATED RAD DOSE IN AIR)
Li⁷F MEASUREMENTS (±10%)
ABSORBED DOSE IN Li⁷F, D(rad)
10³
10²
10¹
10⁰
10⁻¹
-70 -60 -50 -40 -30 -20 -10 0 10 20 30 40 50 60 70
LEFT
RIGHT
ANGLE (milliradians)
1043C5

Fig. 6

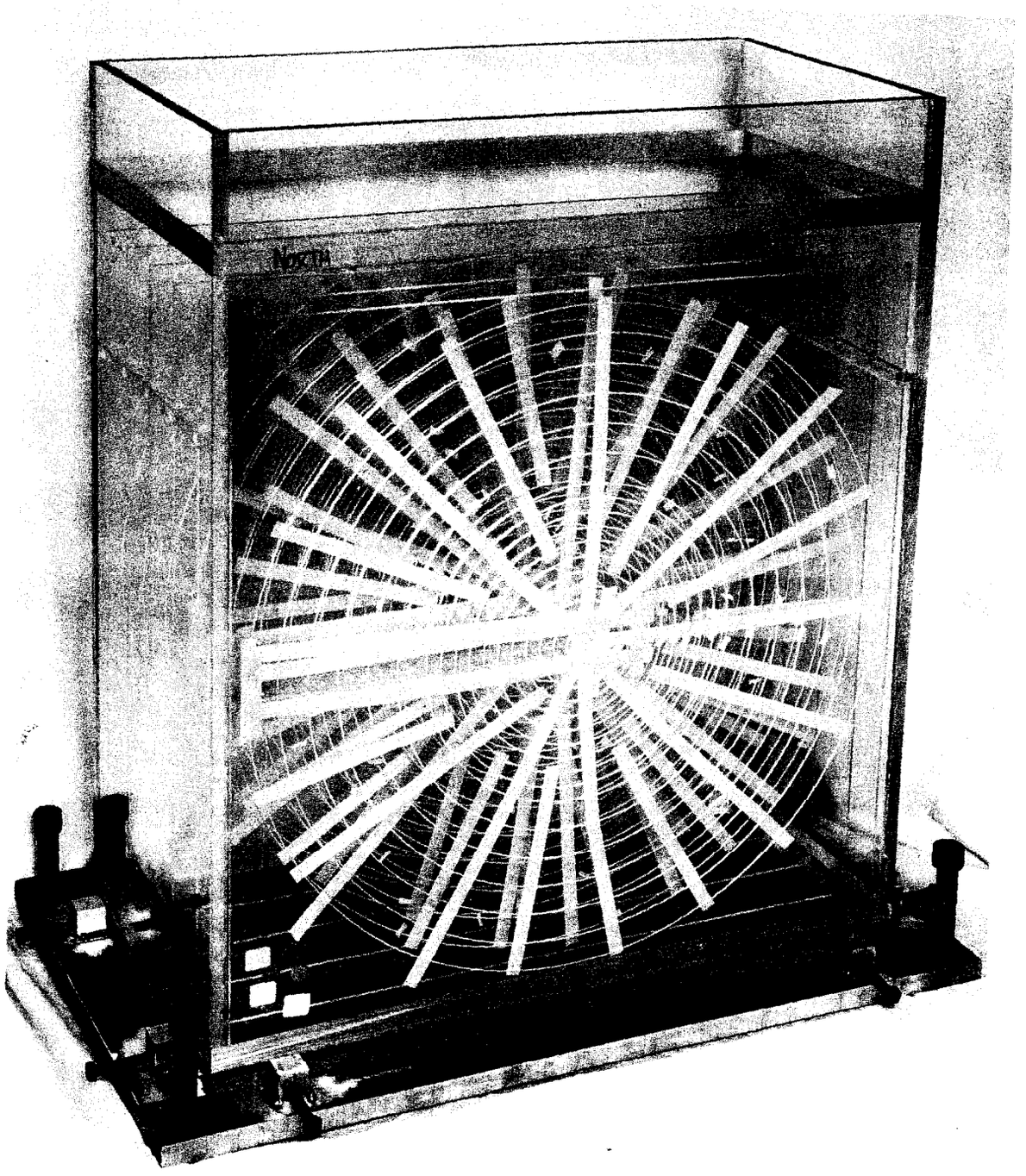

1136A3

Fig. 7

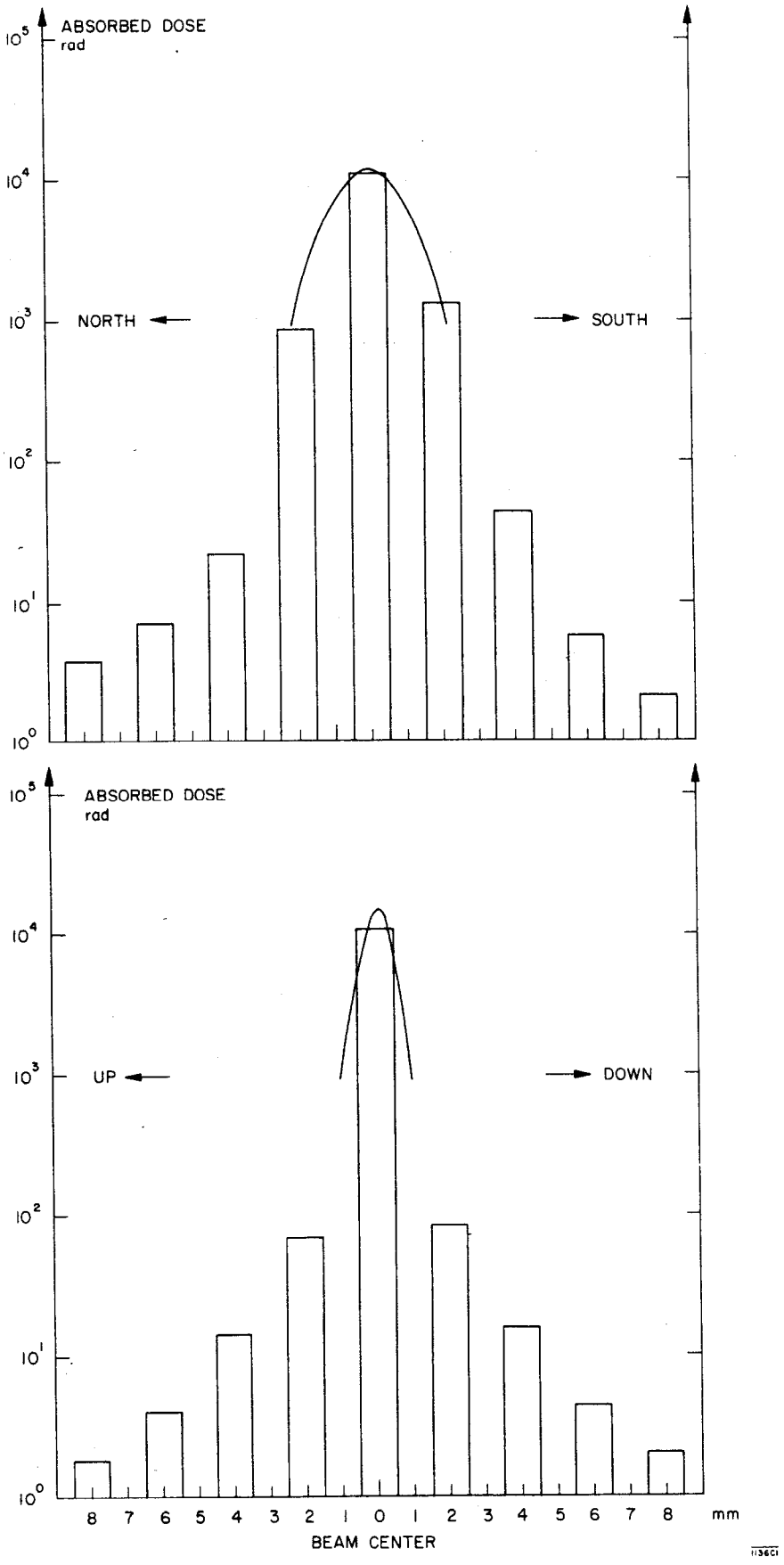
ABSORBED DOSE
rad
10^5
10^4
10^3
10^2
10^1
10^0
NORTH
SOUTH
ABSORBED DOSE
rad
10^5
10^4
10^3
10^2
10^1
10^0
UP
DOWN
8 7 6 5 4 3 2 1 0 1 2 3 4 5 6 7 8 mm
BEAM CENTER
1136C1

Fig. 8